American Mineralogist, Volume 71, pages 343–355, 1986

Lamellar and patchy intergrowths in feldspars: Experimental crystallization of eutectic silicates

JON S. PETERSEN,[1] GARY E. LOFGREN
NASA Johnson Space Center SN4, Houston, Texas 77058

ABSTRACT

Coupled and noncoupled eutectic feldspar intergrowths have been produced by dynamic crystallization experiments in the ternary feldspar–water system. Fractionation during plagioclase crystallization in nearly all compositions examined results in eutectic growth when a solute-enriched boundary layer becomes supersaturated with K-feldspar. The growth rate of the eutectic product generally exceeds that of monophase growth by a factor of 10 or higher and is an effective means of reducing thermal supercooling. Coupled intergrowths have lamellar structures that are normal to a planar, nonfaceted, solid-liquid interface. They are developed predominantly in the {010} crystallographic plane of the host feldspar. The composite crystalline product is usually off-eutectic in composition. Variations in composition occur systematically along the growth direction and across single facets in response to local changes in supercooling. Different crystallographic sectors show systematic compositional differences due to variable nucleation and growth kinetics, which often lead to hourglass patterns superimposed on the intrgrowth structure. Uncoupled eutectic growth occurs in the more K-rich melts. It is a result of the preferential growth of sanidine in the crystallographic **a** and **c** directions and simultaneous, coupled-lamellar oligoclase-sanidine intergrowth in the crystallographic **b** direction. This process leads to a patchy intergrowth with coarse, irregular phase distributions and faceted interfaces. The melt-grown composites have textures strikingly similar to feldspar intergrowths found in cumulus feldspars of the Larvikite monzonite suite in the Oslo igneous province, and this similarity suggests that eutectic growth from near-cotectic melts may account for certain coarse feldspar intergrowths.

INTRODUCTION

Intergrowth textures in igneous rocks, such as quartz-feldspar intergrowths in granophyre and graphic granite, are often compared with eutectic crystallization products in metallic systems. These comparisons have led to the conclusion that certain intergrowth textures form by simultaneous crystallization from the melt (Barker, 1970; Hughes, 1972; Hibbard, 1979; Carstens, 1983). The growth mechanisms and the variable compositions of the intergrowths, however, are not well understood.

Eutectic crystallization has been studied in great detail in metallic systems. Experimental studies in the last two decades have shown not only that eutectic-crystallization products display great variability in growth properties and resulting textures (Chalmers, 1964, chapter 6; Elliott, 1977) but, more importantly, that off-eutectic compositions are common as crystalline products and result from kinetically controlled growth. It is possible to vary the off-eutectic composition by controlling the growth conditions (Mollard and Flemings, 1967a, 1967b; Flemings, 1974, chapters 4, 6).

Experimental studies of eutectic crystallization in silicate melts are difficult because of the strongly anisotropic growth of silicates and the high activation energies associated with nucleation (Swanson, 1977; Lofgren, 1980). Eutectic intergrowth of quartz and feldspar are encouraged by low values of melt entropies for quartz, which reduce tendencies for facet formation (Jackson, 1958), but are complicated by large differences in crystallographic structure. In spite of the difficulties, limited successes in growing these textures from the melt have been reported by Swanson (1976) and Fenn (1979). High-temperature feldspars have high melt entropies but share a common crystallographic structure, which allows an epitaxial relationship between the constituent parts of an intergrowth structure and thus a lower nucleation barrier. Intergrowths of two feldspars therefore should occur more readily than those of quartz and feldspar.

Convincing experimental evidence for simultaneous crystallization of two feldspars from the melt was first reported by Lofgren and Gooley (1977). While the suggestion that composite feldspars could grow from the melt was not entirely new (see review by Smith, 1974, chapter 19), this experimental evidence brought about some debate as to its primary nature (Morse and Lofgren, 1978). Subsequent studies have shown that simultaneous, two-feldspar crystallization occurs spontaneously in a wide range of ternary-feldspar compositions at moderate cool-

[1] Present address: Aarhus University, Aarhus, Denmark.

0003–004X/86/0304–0343$02.00

Table 1. Experimental run conditions, starting compositions, and descriptions of charges

SAMPLE	F1	F7	F11	F10	F9	F8
An	12	20	37	30	19	11
Ab	68	60	45	45	45	45
Or	20	20	18	25	36	44
Wt% H2O	4.0	6.0	10.0	8.0	6.0	4.0
Run No.	601	602	606	605	604	603
Type:	Plagioclase	Plagioclase	Plagioclase	Plagioclase	Plagioclase	glass
Shape:	Branching	Branching	Skeletal	Skeletal	Skeletal	
(875°C)	needles	needles	tabular	prismatic		
Run No.	577	578	582	581	580	579
Type:	Plagioclase	Plagioclase	Plagioclase	Plagioclase	Plagioclase	Composite
Shape:	Branching	Branching	Skeletal	Prismatic	+ composite	Fan-
(800°C)	plates	needles	tabular			spherulitic
Run No.	625	626	630	629	628	627
Type:	Plagioclase	Plagioclase	Plagioclase	Plagioclase	Composite	Composite
Shape:	Branching	Platy	Tabular	Skeletal	Lamellar	Lamellar
(740°C)	platy			prisms	& patchy	& patchy
Run No.	589	590	594	593	592	591
Type:	Plagioclase	Plagioclase	Plagioclase	Composite	Composite	Composite
Shape:	Platy	Skeletal	+ composite	Lamellar	Lamellar	Coarse
(700°C)	fan aggr.	plates	ends	& irreg.	& patchy	patchy
Run No.		635	639	638	637	636
Type:		Composite	Composite	Composite	Composite	Composite
Shape:		Lamellar	Lamellar	Lamellar	Lamellar	Patchy
(650°C)		ends	all sides	& irreg.	& patchy	fan aggr.
Run No.	565	566	570		568	567
Type:	Plagioclase	Composite	Composite		Composite	Composite
Shape:	Coarse	Lamellar	Lamellar		Lamellar	Coarse
(600°C)	fan aggr.	platy	all sides		& irreg.	patchy
Run No	613	614	618	617	616	615
Type:	Plagioclase	Composite	Composite	Composite	Composite	Composite
Shape:	Platy	Lamellar	Lamellar	Lamellar	Lamellar	Coarse
(500°C)	prismatic			prismatic	tabular	patchy

ing rates, and the process must be considered a potential origin for intergrowths of certain types of feldspars as well as other silicate eutectic compositions.

The purpose of this paper is to describe textural features and mineral structures not observed in the earlier study of Lofgren and Gooley (1977) and to present growth mechanisms for the composite intergrowths.

Experimental techniques

Ternary-feldspar starting materials were prepared by the gel method (Luth and Ingamells, 1965), and their compositions are listed in Table 1. Approximately 70 mg of gel was combined with 4–10 wt% triply distilled H_2O and sealed in a platinum capsule. The capsules were weighed after the experiment to check for leaks. The runs were completed in internally heated pressure vessels (Holloway, 1971). The charges were first melted (6–24 h), which produces a uniform liquid. The temperature was decreased either at the linear cooling rate of 2°C/h or in 50°C steps, with the temperature being maintained at each step for 2–3 d. Pressure was approximately 6 kbar during melting, but decreased during cooling according to the *PVT* relations at the constant volume of the pressure vessel to as low as 3 kbar for runs quenched at 400°C. Thermocouples were calibrated against the melting temperature of gold. Polished thin sections of the run products were prepared for textural and chemical studies.

The equilibrium phase relations for the ternary-feldspar system are not well known. The experiments of Yoder et al. (1957) give the general form of the water-saturated liquidus surface at 5 kbar. These data provide a general guide to predict liquidus temperatures of starting materials and the approximate cotectic temperature. The experiments in this study were not all water saturated (at least initially), and the crystal-liquid systems fractionated continuously during the run so that the little we know of the phase relations have only modest application.

A slow (for experimental studies), constant cooling rate of 2°C/h was chosen in order to avoid the growth of highly branching or skeletal crystals. In order to better examine the formation and evolution of the composite intergrowth, the continuous-cooling experiments were interrupted at successive stages of progressive solidification. The successive quench temperatures and textural character of each run are given in Table 1.

Mineral compositions were determined with an automated Cameca three-spectrometer electron microprobe. The microprobe was operated at 15 kV. A 2–3 μm-diameter beam with a sample current of 20 μA was applied to the feldspars, while the glass data were obtained by continuous rastering at 1.6 magnification and 15 μA sample current, in order to avoid excessive Na loss during the measurements. Counting times were 3 × 30 s, and the analyses were calibrated against mineral standards. The technique for analyzing the fine-scale intergrowths is described by Lofgren and Gooley (1977).

Experimental results

Microstructures

The shapes of the feldspar crystals in the products of crystallization correspond broadly to the general patterns previously described (Lofgren, 1974, 1980). Albite-rich plagioclases are predominantly acicular with frequent low-

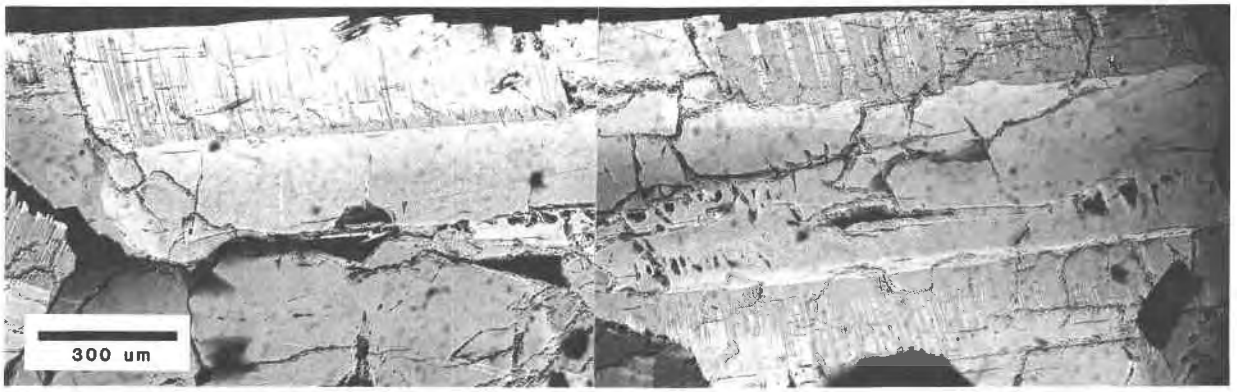

Fig. 1. Lamellar-intergrowth texture along the rim of a normally zoned plagioclase core. The inner, composite zone is dominated by sanidine (dark gray), and the margin, by albitic plagioclase (light gray).

angle branching, whereas the more Ca-rich plagioclases are usually platy or tabular and the more K-rich feldspar compositions tend to have fan-spherulitic shapes. The individual crystal shape, however, changes continuously during progressive solidification as the cores of initially, highly skeletal crystals generally become filled. The irregular external faces of most samples end up as broad facets (see also Lofgren, 1980, Fig. 8) in a process that may be referred to as crystallization ripening. Two or three initially skeletal crystals occasionally fill the entire charge and produce a complex interwoven texture with patchy extinction.

The microstructures described below are mainly from the continuous-cooling experiments, but are equivalent to intergrowth textures in the mainly step-cooled experiments described earlier by Lofgren and Gooley (1977). Two particularly distinct types of intergrowth structures are recognized. The most common is a fine-grained lamellar type comprising 1–10-μm-wide lamellae of albite and sanidine, oriented in a parallel fashion roughly perpendicular to the crystal-liquid interface. The other type consists of coarse, irregular patches of oligoclase in a predominantly K-feldspathic host. These patches are on the order of 20–100 μm wide, substantially coarser than the lamellar type. There is no gradation between these two types, and they often occur in different sectors of a single crystal.

Lamellar-intergrowth structures. Plagioclase crystals in most solidification runs typically have normally zoned cores with a composite rim of lamellar intergrowth (Fig. 1). The lamellae consist of albitic plagioclase in a host sanidine, although often the lamellae and host are of comparable size and proportions. The transition from core plagioclase to sanidine rim is typically discontinuous. The oligoclase lamellae do not have roots in the plagioclase core, but appear within the sanidine some few micrometers from the transition interface (Fig. 1).

Another characteristic feature of the lamellar intergrowth is the compositional variation toward one end member along the growth direction. Narrow albite lamellae in the inner, sanidine-rich product become increasingly wider outward and grade into an albite-rich plagioclase rim with planar and faceted crystal interfaces (Fig. 2). More rarely, the compositional variation terminates with a K-rich composition. By contrast, the solid-liquid interface of the composite product is often ragged in detail, although it appears macroscopically planar.

In addition to the systematic compositional change in the growth direction, a complete textural variation from monophase plagioclase through intermediate sections with near-equal proportions of oligoclase and sanidine to monophase sanidine is occasionally observed across single crystal faces. This variation shows that the growth conditions also differ along single growth planes (Fig. 3).

The influence of crystallography on the growth morphology is revealed by the different textural characteristics of the lamellar intergrowths in different growth sectors. In the {010} plane the microstructure is usually regular and consists of oligoclase and sanidine in lamellar or rod-shaped intergrowths. The solid-liquid interface is planar,

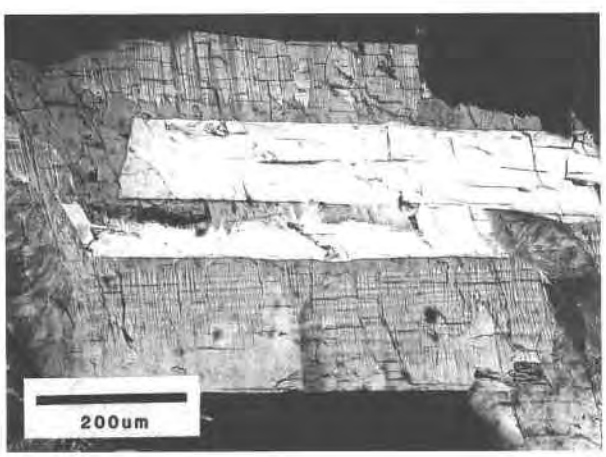

Fig. 2. Continuous cooling experiments show a marked, discontinuous appearance of sanidine (dark gray) at the plagioclase interface and gradually diminishing amounts outward at the expense of plagioclase. Transverse banding is the result of minor growth disturbances.

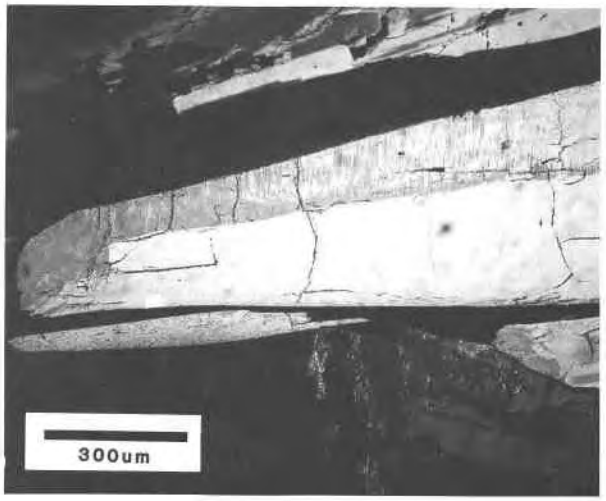

Fig. 3. Gradual compositional changes along single crystal facet. Sanidine is dark gray; oligoclase, light gray.

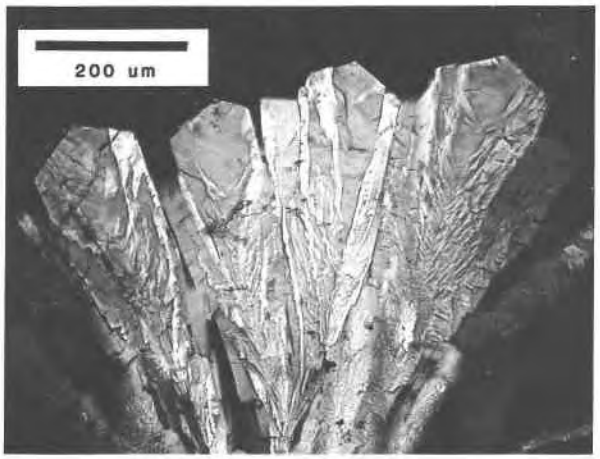

Fig. 4. Patchy intergrowths become increasingly coarse in the growth direction. Dark gray is sanidine; light gray, oligoclase with minor amounts of K-feldspar. Note colony structure and feather pattern.

though the lamellae are often not exactly perpendicular to the plagioclase substrate but deflected at a finite angle. In the {001} plane, on the other hand, the structures are much more irregular, and the ratio of the two constituent phases highly variable. The solid-liquid interface of this type is usually nonplanar, and the second phase may be rod shaped, vermicular, irregular, or platy.

Patchy-intergrowth structures. Patchy intergrowths—which seem to be confined to the most K-rich starting materials, F-8 and F-9—are characterized by a substantially coarser grain size and irregular appearance. Individual patches measure from 10 to over 100 μm across. The product is dominated by K-feldspar over plagioclase in a ratio of about 2:1 or higher. Feldspars with patchy intergrowths usually form a characteristic colony structure (Fig. 4). Individual crystals are aligned in parallel bundles that tend to expand in width along the growth direction and produce a radiating rosette structure consisting of numerous individual crystal subgrains. Because of their simultaneous formation, these subgrain aggregates often form a compact cellular structure with a curved growth structure projecting toward the most nourishing residual melt (Fig. 5). Only the ends of the parallel feldspars are exposed to unhindered growth and form well-developed facets, unlike the lamellar composites. The nonorthogonal appearance of the facets shows that the faceting planes are {001}-{101} or {110}-{110}, thus following crystallographic **a** and **c** directions (Fig. 4).

Within the crystal subgrains are two feldspar components intergrown in a patchy structure. The central stem is usually dominated by sanidine, whereas plagioclase appears near the margins. Because of the expanding nature of the growth, the plagioclase patches project toward the central stem and create a featherlike structure (Fig. 3). Mutual, internal boundaries between the component phases in this type of intergrowth are irregular and noncrystallographic. The elongation of individual patches is usually at low angles to major crystallographic planes or facets when such are developed (Fig. 4).

Mineral compositions

Results of microprobe analyses of the synthetic feldspars are presented in Table 2. The compositional range of representative, single feldspars in each group is given together with the co-existing glass, represented by the average of 5–10 points. The totals of the glass analyses are low, about 96 vol%, owing to dissolved water (analyses in Table 2 have been recalculated to 100% for comparison with starting material). Presence of free vapor bubbles indicate that most runs were water saturated when the experiments were terminated.

Plagioclases in the most An-rich composition (F-11) show the widest range of compositional zoning before the appearance of composite growth (Fig. 6a). The initial feldspar (crystal core) is labradorite, about An_{75}. In the experiments cooled down to 740°C, the crystal-melt system has fractionated so that the rim is andesine (An_{45}) and at 700°C, oligoclase (An_{30}). In this range, the orthoclase component increases from less than 1 to 5 mol%, which is within the solubility range of plagioclase feldspars (Smith, 1974). At 650°C, the plagioclase rim compositions are about An_{25}, but here some sectors have composite rims with an outer margin of about $An_8Ab_{77}Or_{15}$. Because of the systematic compositional variation along the growth direction, the overall composition of the composite rim is less Or-rich than the innermost composite section, which may be as high as $An_2Ab_{30}Or_{68}$ (Fig. 6b). Average melt compositions at the time of appearance of composite growth corresponds to $An_{15}Ab_{43}Or_{42}$.

Initial plagioclase compositions in F-10 are roughly identical to those of F-11 at 875°C, as is the overall range of zoning. At 740°C, the feldspars in the two charges are virtually identical, whereas in F-10 at 700°C a composite margin forms on the oligoclase rim. This margin is ini-

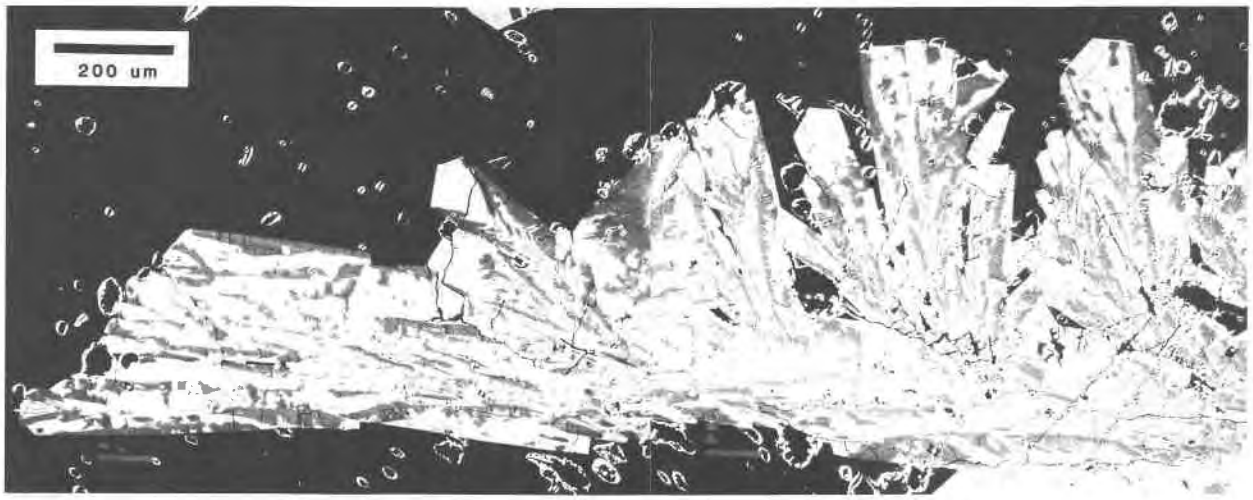

Fig. 5. Preferential growth along the horizontal axis of patchy products; continuous widening of individual colonies forces growth away from the principal growth plane in a fan-spherulitic manner. Back-scattered electron image.

tially K-rich with an average about $An_3Ab_{21}Or_{76}$, which grades outward to a more intermediate composition of $An_9Ab_{40}Or_{51}$. In the subsequent 650°C sample, the rim has fractionated to $An_{17}Ab_{52}Or_{31}$. The melt composition at the time the composite rim forms has a An:Ab:Or ratio of 16:36:48, roughly equivalent to that of the previous charge at the equivalent stage of fractionation.

The F-8 samples show no initial plagioclase precipitation and no crystalline phases at 875°C. The early components of the composite crystals measure $An_{28}Ab_{59}Or_{12}$ and $An_4Ab_{27}Or_{69}$, respectively, at the solid-liquid interface. Integrated analyses at various positions in the elongate crystals show minor variations except for a slight decrease in the Ca content along the growth direction (Fig. 6c).

Because of the fine lamellar intergrowth, minor amounts of sanidine are included in most plagioclase analyses, and the data tend to plot on the Or side of a mixing line between ideal plagioclase and sanidine (Fig. 6b). The discontinuous appearance of sanidine on the plagioclase core allows better definition of the Or-rich component of the intergrowth. If the crystallization product is exclusively a composite, the plagioclase component varies from An_{32} in the root zone to An_{18} in the marginal portion of single crystals (Fig. 6c). The changing composition of coexisting feldspars is in accordance with decreasing temperature.

Melt fractionation

The melt compositions vary in accordance with the crystallizing phase assemblage; during initial plagioclase precipitation, the residual melt becomes enriched in Na and K following the expected liquid line of descent toward the cotectic field boundary (Fig. 7). At the appearance of sanidine and subsequent composite growth, this trend becomes deflected toward the eutectic minimum. The deflection point, however, is systematically displaced toward the An-Ab join and significantly above the equilibrium cotectic boundary at 5 kbar according to Yoder et al. (1957). This occurs because solute accumulates in the boundary layer at the liquid-solid interface which produces local conditions favorable for sanidine nucleation

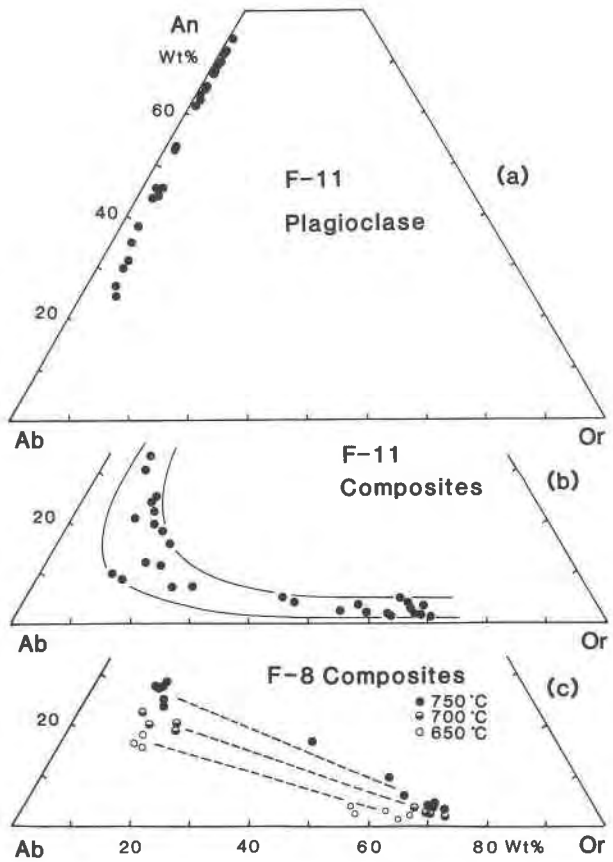

Fig. 6. Microprobe analyses of minerals grown from starting materials F-11 and F-8.

Table 2. Electron-microprobe analyses of feldspars and glasses in experimental charges

OXIDE	F-8	627GL	627PL	627KF	591GL	591P1	591K2
SiO_2	64.17	66.46	60.65	64.37	69.75	62.39	65.28
Al_2O_3	20.84	21.82	24.31	19.31	22.44	23.66	19.39
CaO	2.20	2.07	5.68	0.60	1.65	4.73	0.58
Na_2O	5.35	3.59	7.22	2.84	2.56	8.01	3.25
K_2O	7.45	6.05	1.90	12.27	3.59	2.05	11.81
TOTAL	100.01	99.99	99.76	99.39	99.99	100.84	100.31
An	11	13.1	27.0	3.0	15.7	21.8	2.8
Ab	47	41.2	62.2	25.3	43.9	66.9	28.7
Or	43	45.7	10.8	71.8	40.4	11.2	68.5

OXIDE	636GL	636P1	636K3	F-10	605GL	605P3	605P7
SiO_2	69.50	65.09	65.06	60.09	61.79	50.48	51.45
Al_2O_3	23.52	22.31	19.33	24.33	23.92	31.19	30.72
CaO	0.81	3.30	0.23	6.04	4.77	14.02	13.55
Na_2O	3.05	7.05	3.89	5.34	4.65	3.42	3.76
K_2O	3.12	2.14	11.22	4.20	4.87	0.24	0.26
TOTAL	100.00	99.89	99.73	100.00	100.00	99.35	99.74
An	8.1	17.7	1.1	29.0	25.1	68.0	66.0
Ab	54.9	68.6	34.1	47.0	44.3	30.0	33.0
Or	37.1	13.7	64.8	24.0	30.6	1.4	1.5

OXIDE	629GL	629P4	593GL	593C1	593P2	638GL	638P1
SiO_2	63.53	52.04	68.12	63.49	52.06	66.48	51.89
Al_2O_3	23.36	30.44	21.45	20.62	30.44	22.64	31.07
CaO	2.95	12.95	2.25	1.99	12.94	0.94	13.17
Na_2O	3.94	4.06	2.72	4.11	3.88	4.84	3.97
K_2O	6.20	0.33	5.45	9.26	0.29	5.08	0.33
TOTAL	99.98	99.82	99.99	99.47	99.61	99.98	100.43
An	16.9	62.6	16.5	9.7	63.7	6.0	63.5
Ab	40.8	35.5	35.9	36.4	34.6	55.9	34.6
Or	42.3	1.9	47.6	53.9	1.7	38.4	1.9

OXIDE	638K1	F11	606GL	606P5	606P8	630GL	630P1
SiO_2	65.47	58.57	61.47	51.80	49.10	65.11	58.36
Al_2O_3	19.25	25.59	24.52	31.13	32.83	23.31	26.57
CaO	0.22	7.45	5.54	13.29	15.31	2.85	7.96
Na_2O	3.69	5.35	4.61	3.85	2.80	3.62	6.88
K_2O	11.57	3.05	3.85	0.21	0.13	5.11	0.61
TOTAL	100.20	100.01	99.99	100.28	100.17	100.00	100.38
An	1.1	36	30.0	64.8	74.6	18.4	37.7
Ab	32.3	47	45.2	34.0	24.7	42.3	58.9
Or	66.7	17	24.8	1.2	0.7	39.3	3.4

OXIDE	630P5	594GL	594P3	594P6	639GL	639C1	639P3
SiO_2	51.30	66.67	50.77	61.58	66.68	65.65	60.38
Al_2O_3	31.73	22.04	32.00	24.04	22.76	18.96	25.45
CaO	13.94	2.29	14.24	5.90	1.07	0.16	6.33
Na_2O	3.57	3.59	3.35	7.22	4.77	3.33	6.48
K_2O	0.19	5.39	0.16	0.90	4.71	12.04	1.20
TOTAL	100.73	99.99	100.52	99.64	99.99	100.14	99.84
An	68.0	15.0	69.5	29.4	7.0	0.8	32.5
Ab	31.0	42.8	29.6	65.2	56.4	29.4	60.2
Or	1.1	42.2	0.9	5.4	36.7	69.9	7.3

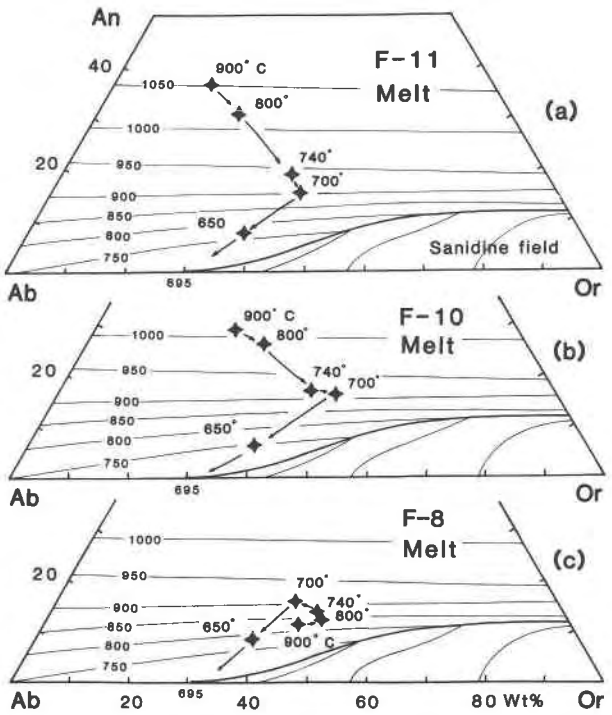

Fig. 7. Microprobe analyses of average glass compositions at various stages of solidification in starting materials F-8, F-10, and F-11. Isotherms from Yoder et al. (1957) emphasize the nonequilibrium nature of the experimentally produced liquids.

and subsequent composite growth before the bulk melt reaches cotectic composition. Once formed, however, the modal proportions of the constituent phases in the composite product are determined only by the degree of supercooling and the rate of advance of the interface. The residual-liquid fractionation trend therefore reflects the kinetic conditions rather than continued differentiation toward the cotectic minimum. In near-cotectic melts such as F-8 (Fig. 7c), the composite product may therefore initially drive the coexisting melt away from the cotectic thermal minimum, as a result of preferential growth of sanidine over plagioclase. After a transient period this trend becomes stabilized and is redirected toward the eutectic minimum for the system (Fig. 7c).

The timing and formation of composite growth in the ternary-feldspar system are thus closely related to melt composition. Analyzed feldspars in a series of successive samples of composition F-10 illustrate the evolution of the contemporaneous solid and liquid in terms of Ca and K redistribution (Fig. 8). Initial plagioclase crystallization depletes the melt in Ca, whereas the corresponding enrichment in K eventually leads to supersaturation with respect to sanidine resulting in composite growth. The nucleation and growth of sanidine affect the residual liquid with respect to K in the same manner as Ca was affected by the earlier plagioclase fractionation. An interesting effect, however, is created by this process: Ca is enriched in the solid as the fraction of plagioclase in the composite increases outward. This creates an inverse zonation with increasing Ca outward and produces a plagioclase rim on the K-feldspathic composite. This feature is similar to that in the so-called rapakivi texture, but opposite to that expected from equilibrium-crystallization conditions.

In the most K-rich, near-cotectic melt composition (F-8), plagioclase is not the first phase to precipitate. Instead,

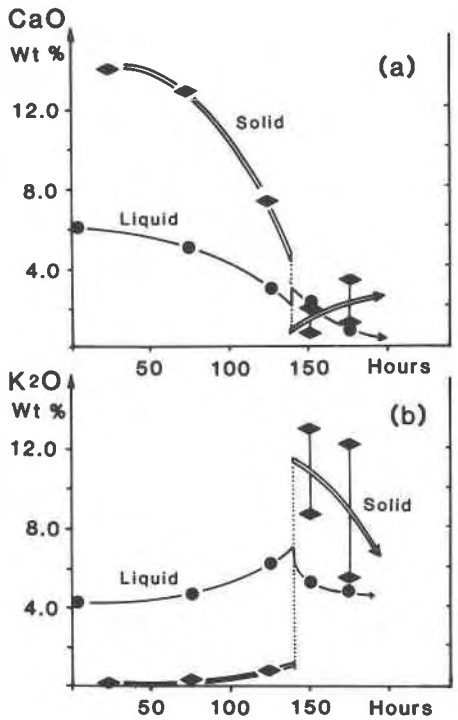

Fig.8. Evolution of contemporaneous melt and solid compositions during progressive fractionation in starting material F-10; (a) shows the CaO and (b) the K_2O distribution. The discontinuous solid trends occur when a composite phase nucleates and starts growing.

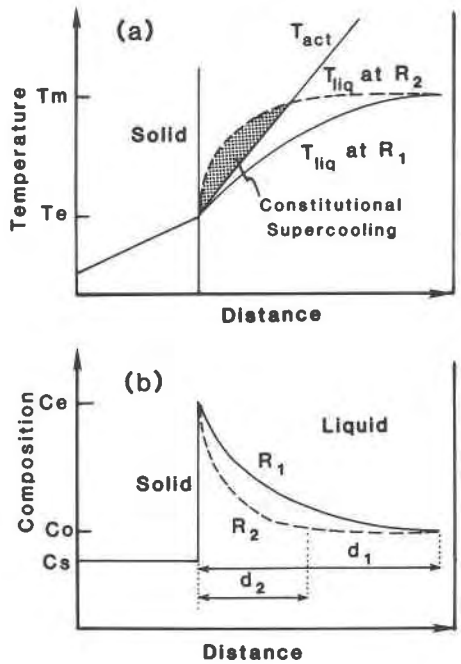

Fig. 9. (a) Relations between growth rates, $R_1 < R_2$, and the corresponding liquidus-depression curves; (b) the diffusive boundary layers are d_1 and d_2, respectively. T_e and C_e are eutectic temperature and composition, and T_m and C_o, initial melt temperature and composition.

albitic plagioclase and sanidine apparently precipitate simultaneously, side by side, and because this assemblage is closer to the melt composition than each of the individual phases, there is little liquid fractionation. Dominant growth of K-feldspar initially enriches the liquid slightly in plagioclase components, but after a transient period, the eutectic growth is stabilized and brings the residual liquid toward the eutectic minimum. The duplex crystallization is therefore maintained throughout the solidification range. By contrast, the most albite-rich composition, F-1, never precipitates a separate K-rich phase during the course of crystallization. It appears that the more Na-rich (and Ca-rich) the melt, the greater must be the fraction crystallized before composite growth is observed; i.e., the further the melt composition is removed from the cotectic, the more the liquid must fractionate to reach the conditions for composite intergrowth.

Eutectic solidification

The composite feldspar intergrowths have many features in common with eutectic solidification structures described in the metallurgical literature. A brief discussion of eutectic solidification mechanisms is therefore included here. A prime condition for simultaneous, coordinated growth of two phases is that the solute enrichment in the boundary layer is sufficiently small to prevent constitutional supercooling for a given temperature gradient, yet high enough to produce a boundary layer with eutectic composition at the solid interface (Mollard and Flemings, 1967a; Flemings, 1974, p. 94). These conditions are met with a comparatively slow solidification rate (R_1 in Fig. 9b), where the accumulated solute is distributed over a comparatively wide diffusion zone (d_1), and the temperature gradient (T_{act}) is steeper than the tangent to the liquidus-depression curve (T_{liq}) at the interface (Fig. 9).

Eutectic growth is termed "coupled" when the composite solidification occurs with a planar front; that is, the growth is coordinated so that neither phase grows faster than the other, and the combined growth is faster than each of the constituent phases alone (Rutter, 1977). Once the composite product is formed, a planar, nonfaceted interface is stabilized by transverse diffusion between the constituent phases. This diffusion range is on the order of one-half interlamellar spacing, and very different from the long-range diffusion in the solute-enriched boundary layer, which may have initially led to the duplex nucleation.

Experimental and theoretical studies show that the composition of the composite product is related to solidification rate (Mollard and Flemings, 1967a, 1967b). Ideally, when both the solid and the liquid have exactly a eutectic composition, solute is redistributed and immediately consumed at the solid interface by the two phases, and there is no boundary layer. In this special case, changing growth rates clearly will not affect the overall composition. However, significant changes in the interface

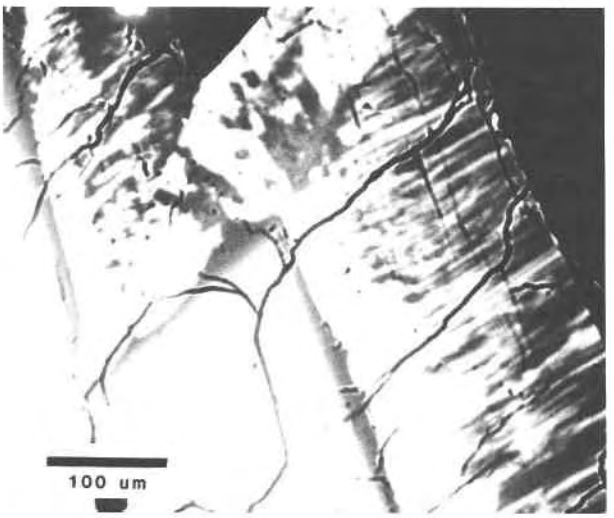

Fig. 10. Back-scattered electron image of lamellar intergrowth showing sector zoning and gradual compositional changes. K-feldspar is white; albitic plagioclase, dark gray; glass, black.

velocity will remove the average solid composition substantially from the eutectic, provided the conditions for a plane-front solidification are maintained (Mollard and Flemings, 1967a; Hunt and Jackson, 1967). When the solid is removed from eutectic composition, residual solute accumulates in a diffusive boundary layer. This boundary layer, being on the order of D_L/R wide (Flemings, 1974, p. 109) where D_L is the diffusion coefficient in the liquid and R the growth rate, can be affected by convective flow unlike the much narrower transverse diffusion zone which is largely within the static portion of the boundary layer. Because the composite interface is isothermal, changes in growth rate or thickness of the nonconvective boundary layer will therefore result in compositional changes in the composite product that follow a plane-front solute-redistribution pattern (Mollard and Flemings, 1967a). This can result in gradual compositional changes, steady-state growth, or compositional banding following Tiller et al. (1953).

The structure of eutectic composites is generally lamellar or rod shaped, depending on the proportion of the secondary phase (Mollard and Flemings, 1967b; Elliott, 1977). A volume fraction of $1/\pi$ marks the theoretical stability of rod morphologies although experimental data suggest even lower values because of anisotropic surface energies of the constituent phases (Flemings, 1974, p. 104). Faceting behavior of one phase leads to more complex patterns that reflect the anisotropy of the faceting phase (Hunt and Hurle, 1968; Croker et al., 1975a, 1975b).

Discussion: Origin of the intergrowths

Lamellar intergrowth

Evidence of coupled eutectic solidification with lamellar structures is seen in many of the composite feldspar zones. Usually, the lamellar intergrowth is bounded by planar interfaces. A conspicuous banding in some growth sectors, produced by fluctuations in composition along the solidification front (Fig. 2), shows that a roughly planar solidification front is also present during growth of the composite product. The occasional, regular deflection of lamellae from a direction perpendicular to the solidification front indicates departure from an isotropic or continuous growth mechanism, possibly created by the presence of facets in one of the constituent phases along the liquid groove between two adjacent phases (Hunt and Hurle, 1968; Morris and Winegard, 1969).

The lamellar intergrowth is formed when the solute-enriched boundary layer at the growing plagioclase interface becomes supersaturated with K-feldspar, which nucleates and starts growing. The subsequent heterogeneous nucleation of albitic plagioclase on this sanidine has a low energy barrier because of high structural compatibility (Lofgren, 1983) and therefore occurs readily as the boundary layer becomes depleted in K and enriched in Na. From then on, the combined growth of the two phases is stabilized by transverse diffusion, which provides nutrients for the complementary phases and results in a more rapid growth rate. The discontinuous appearance of sanidine on the plagioclase core as opposed to the continuous appearance of albite lamellae in the K-feldspar suggests that the nucleation of sanidine on a plagioclase host apparently has a higher energy barrier than the precipitation of albitic plagioclase on K-feldspar.

Systematic changes in the composition of the solid product during progressive growth (zoning) are the result of gradually changing solidification conditions. When the isothermal growth is unable to keep up with the continuous cooling rate, the interface becomes increasingly supercooled and gradually changes composition toward a more albitic plagioclase end member (Fig. 10). Furthermore, since the liquidus depression is greatest at the central portion of large facets (because of the edge effect on solute distribution), the instantaneous supercooling will be highest there, and the bulk composition will accordingly be more Ab rich than the composite formed simultaneously near the edges. Observed textures and compositional relations clearly support this view (Figs. 1, 3).

The composition of the composite product also varies with crystallographic direction. In the elongated, faster-growing direction of the feldspar crystals, the solid is systematically more potassic than in the flattened {010} sector. This pronounced difference in composition must result from different growth properties in different crystallographic directions. Dowty (1976a, 1976b) emphasized the influence of crystal structure on morphology and sector zoning, and, adding the influence of different conditions for heterogeneous nucleation of a secondary phase in different lattice planes (the wetting factor), the prominent differences can be ascribed to crystallographic factors. The optical continuity of host and lamellae in different growth sectors of single crystals suggests that there is an epitaxial relationship between the host and product phases. This allows principal crystallographic properties to be maintained in the different directions

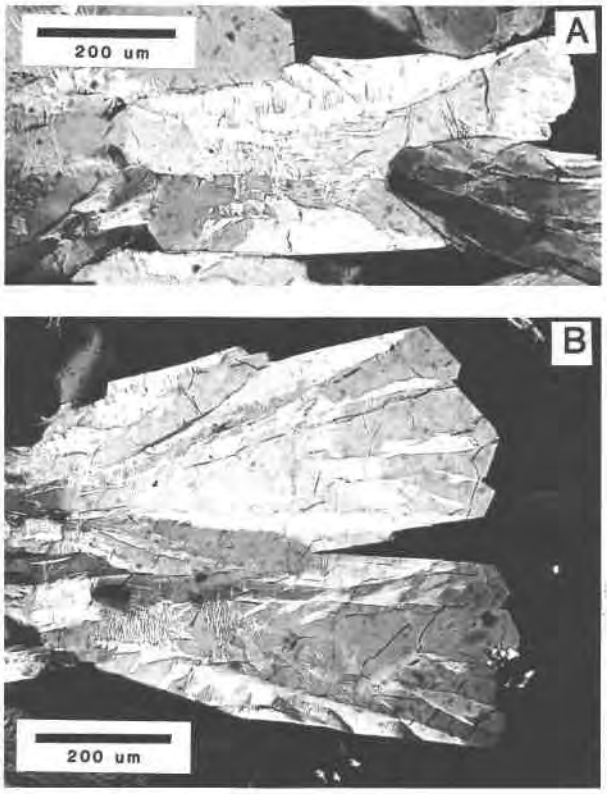

Fig. 11. Sectoral distribution of patchy intergrowths. (a) Lamellar structures dominate the {010} crystallographic plane, while K-feldspars dominate the **a**-**c** crystallographic plane. (b) Faceted growth in crystallographic **a** and **c** directions is predominantly K-feldspar (dark), while lamellar intergrowths (light) form the sides of each subgrain. Note the lamellar character of the structures at the base of the feldspar colony when a composite sector is cut perpendicular to the growth direction.

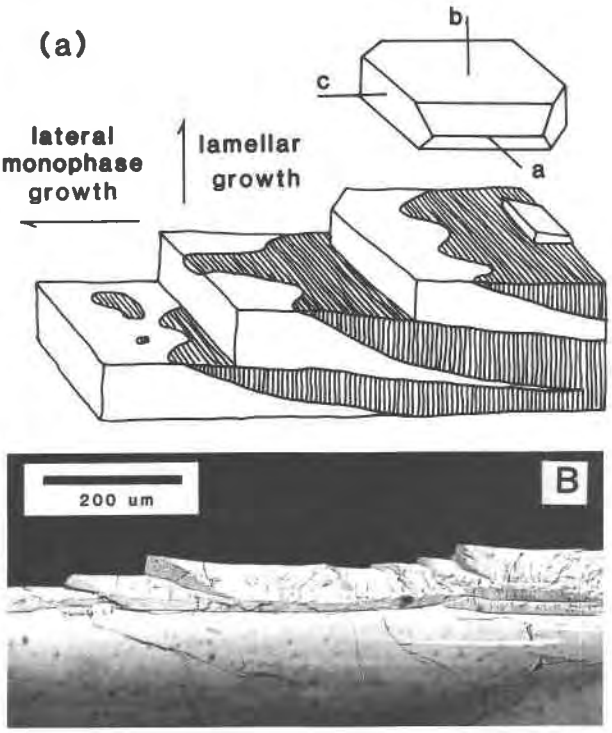

Fig. 12. (a) Schematic presentation of the patchy-intergrowth configuration in relation to main crystallographic planes of a monoclinic feldspar. Rules represent lamellar intergrowth; white parts are the leading sanidine. Facets may or may not develop on the leading edge of a growth subunit. If the sanidine zone expands simultaneously in two directions, a cuneiform-intergrowth pattern (as seen in Fig. 5 of Lofgren and Gooley, 1977) is formed. (b) Equivalent relations in a synthetic feldspar. Sanidine (dark gray) grows preferentially in lateral (horizontal) directions, whereas a composite, oligoclase-rich product (light gray) dominates the vertical growth, normal to the interface.

during composite growth and commonly leads to an hourglass pattern superimposed on the intergrowth.

A convex interface with a radiating lamellar structure, as seen in many end sectors, shows that growth of sanidine is leading slightly over plagioclase in this direction (Jackson and Hunt, 1966). If this difference in growth rate of the two components increases even more, e.g., because the differential growth anisotropy increases further with changing supercooling (Jackson, 1984), coupled growth can no longer be maintained, even with the convex interface. Only a single phase will precipitate in this particular crystallographic direction, whereas composite growth is maintained in other directions. The relationship between composite structures in different sectors and overall melt differentiation in the studied samples is significant and is covariant with supercooling. In the most K-poor samples, composite growth occurs only in the elongated **a** or **c** crystallographic directions. In more evolved stages of solidification, when the K content of the melt is sufficiently high to provide conditions for composite growth in the {010} planes, the correspondiing {001} sectors are usually monophase sanidine.

Patchy intergrowths

The formation of patchy intergrowth results from an entirely different growth mechanism than the lamellar type. The irregular distribution of the constituent phases shows that this growth is uncoordinated; one phase grows structurally independently of the other. As the solidification proceeds there is a significant coarsening of the patchy intergrowth. Initial phase segregations on the order of 10-μm width increase to broad areas more than 100 μm wide. The solid-liquid interface of the individual patches often shows facets, usually bounded by {001}-{101} planes and with maximum elongation along **c**. Two phases may share a common facet plane, but more often sanidine dominates facets in the elongated direction whereas albitic plagioclase and/or composite lamellar products dominate the sides or flanks of elongated crystal branches (Fig. 4). Patches of faceted sanidine and lamellar plagioclase-sanidine composites often co-exist in single crystals (Figs. 11a, 11b).

The following growth model for the patchy intergrowth is proposed. Heterogeneous nucleation of sanidine occurs epitaxially on a facet of a normally zoned plagioclase crys-

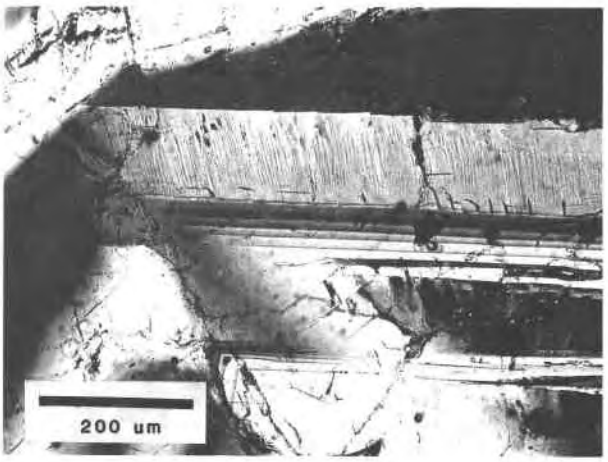

Fig. 13. Step-cooled feldspars with discontinuous growth zones. The composite zone is notably wider than the inner, monophase zones.

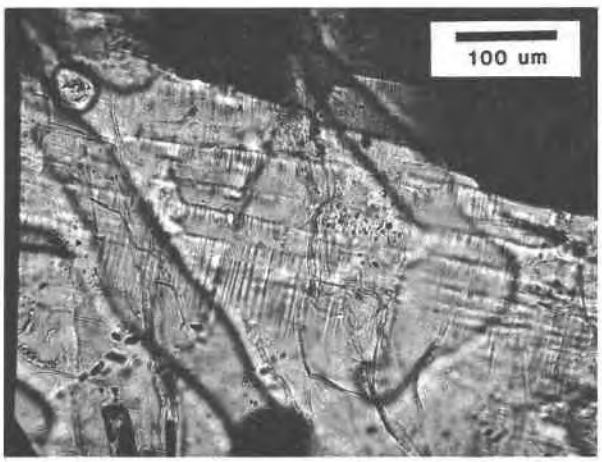

Fig. 14. Lamellar intergrowth with a rhythmic, banded structure due to the discontinuous appearance of albitic plagioclase lamellae in a predominantly K-feldspathic host.

tal. Growth of this sanidine in the {010} direction eventually results in a coupled, lamellar plagioclase-sanidine intergrowth as discussed above, with the lamellae projecting away from the interface. The simultaneous spreading of growth layers is influenced by the diffusive boundary layer created by the pre-existing plagioclase facet; i.e., the lateral, edgewise growth projects into a liquid that is already enriched in low-temperature components (Figs. 12a, 12b). The growth in this direction may thus occur as a noncoupled, eutectic solidification, where the re-entrant angle of the growth step creates a stable phase boundary. This process is enhanced by anisotropic growth factors that encourage the growth of sanidine in the crystallographic **a** and **c** directions.

Since the lateral and the perpendicular growth occurs simultaneously, the composite sector gradually returns toward albitic plagioclase while simultaneous sanidine precipitation occurs in the lateral growth front. At some stage, renewed nucleation of sanidine will occur on top of the composite plane and start spreading a new layer. By this time the sanidine transgresses the composite product of the previous layer, and the conditions for its further growth are diminished (Fig. 12a). Clearly, the above process can occur repeatedly and lead to overlapping zones of composite and noncomposite products, creating a highly irregular phase distribution. The growth process is comparable to layer speading and may lead to faceted crystals (Fig. 12b).

The patchy intergrowth occurs because the growth rate of the sanidine exceeds that of the composite product in the crystallographic **a** and **c** directions, and a plane front cannot be maintained. In this case, the one phase grows rapidly into the melt while the other precipitates at some distance behind. When fast growth is directed in the elongated direction of the host crystal, slower growth in the transverse direction occurs simultaneously with a plane front and forms a coupled eutectic structure.

Growth rates

Planar interfaces intuitively suggest growth by layer spreading controlled by interface attachment kinetics. The planar interfaces of lamellar eutectic structures, however, are the result of the isothermal character of the composite growth mechanism, which exceeds the rate of faceted growth by layer spreading by many orders of magnitude (Flemings, 1974, p. 95; Rutter, 1977). Growth by layer spreading occurs by surface-edge nucleation or screw dislocation and is usually controlled by the nucleation rate of new layers (Kirkpatrick, 1981). The latter is slightly faster for a similar degree of supercooling because it has no nucleation barrier, and in the case of increasing supercooling, the screw dislocation may dominate the growth (Gilmer, 1977; Kirkpatrick, 1981). Substantially faster growth rates, however, are achieved when supercooling exceeds the roughening temperature of certain facets, and the solid interface becomes atomically rough (Gilmer and Jackson, 1977; Hartman, 1982). In this case, a planar solid-liquid interface reflects the isotherms along the solidification front. The rate of growth in this case is controlled only by the rate of attachment of constituent components to the interface and removal of expelled solute by diffusion. In coupled eutectic growth, this rate-limiting accumulation of solute is minimized since the neighboring phases consume complementary solute and thus mutually encourage their growth by transverse diffusion. This reduces the boundary-layer width and allows very high solidification rates because the rate-controlling diffusion range is reduced to the order of the interlamellar spacing.

Coupled eutectic growth accordingly predicts a dramatic increase in the solidification rate when compared with the growth of single phases. This is most clearly seen in step-cooled experiments, where the temperature is dropped 50°C for constant time intervals of 2 d. Each temperature drop creates a new growth zone whose width reflects the relative growth rate for each time interval.

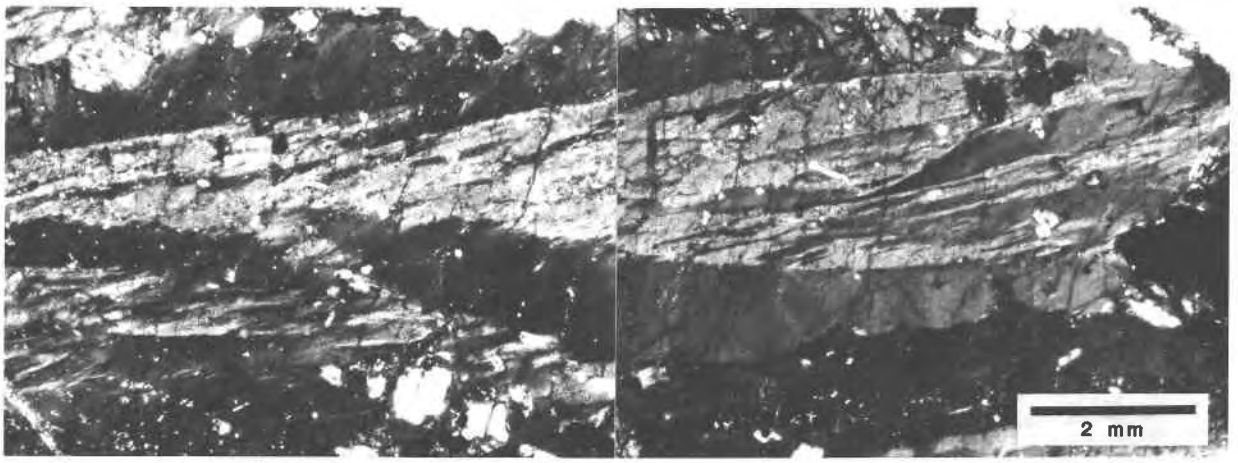

Fig. 15. Natural, patchy intergrowth of two feldspars in comb-textured lardalite feldspar. Photomicrograph shows the tip of a columnar feldspar with maximum elongation in crystallographic **b** direction. K-feldspar grows preferentially laterally (dark gray); the lighter-gray central stem is flame-structured oligoclase.

Because of the closed-system fractionation, the residual liquid becomes fractionated and ultimately reaches the conditions for cotectic crystallization. At this stage a dramatic change in the growth conditions leads to a composite growth zone more than ten times wider than the previous monophase zones (Fig. 13). This fact emphasizes the unique nature of the coupled eutectic growth and severely restricts the possibility that the intergrowths may have precipitated as homogeneous phases and later exsolved into a two-phase product.

Because the products of eutectic crystallization often solidify with off-eutectic compositions, a limited boundary layer is usually present and affects the solid composition. As the off-eutectic solid composition shifts toward one end member under supercooled conditions, it may pass the extension of the liquidus curve of the other phase. Thus being outside the maximum solubility range of this phase, it ceases growth, and a monophase precipitation temporarily takes over. As this creates complementary solute enrichment in the boundary layer, the process can repeat itself, creating a banded structure, as often seen in some metal eutectics (Hurle and Hunt, 1968). Compositional variations showing cyclic appearance of monophase bands in the growth direction are occasionally observed in the composite feldspars. One such case of rhythmic variations that could be the result of this mechanism is shown in Figure 14.

Application of results to natural feldspars

The wide range of crystallization conditions that produce eutectic structures in the experiments with ternary-feldspar melt compositions suggests that conditions for similar growth behavior would be expected in natural rocks. Owing to extensive solid-state transformations and exsolution in the natural feldspars, however, the structures may not be readily recognized.

Eutectic solidification is primarily a result of growth at moderate to low supercooling rather than high supercooling, and the formation of composite intergrowths thus is expected to occur in plutonic rather than in volcanic environments. The existence of a complete solid solution for K- and Na-rich feldspars at low pressures (Morse, 1968) further restricts the occurrence in volcanic rocks and favors its occurrence primarily in plutonic rocks.

Plutonic feldspars with complex intergrowths are reported by Barth (1945) from monzonitic larvikite occurrences in the Oslo region, Norway. The two components of this intergrowth are plagioclase, An_{17-25}, and alkali feldspar about $An_4Ab_{48}Or_{48}$, which are equivalent to the components of eutectic intergrowths reported in the present experimental study. Oftedahl (1948) recognized patchy intergrowths in some of the more calcic members of the same rock series and ascribed them to primary growth. Despite these interesting observations, subsequent studies of larvikite feldspars have focused mainly on the spectacular and intricate alkali feldspar unmixing patterns, believed largely to derive from solid-state reactions (Muir and Smith, 1956; Smith and Muir, 1958; Smith, 1974). The influence of late, solid-state reactions, however, would not destroy any primary intergrowth, but rather enhance it and possibly smooth the initial phase boundaries. In view of the present results, therefore, a significant contribution to unusually coarse segregation in these feldspars could result from primary growth. Strong support for this view comes from an occurrence of comb-layered feldspars in the Lardalite intrusion (Petersen, 1985). The lardalite is a nepheline-rich variety of the larvikite, and the feldspars are clearly related though they are slightly more Or-rich in lardalite than typical larvikite. The feldspars in these contact zones grow parallel to one another in a columnar fashion perpendicular to the intrusion border (Petersen, 1985). Their lateral growth is constrained by neighboring crystals and the feldspars are elongated in the crystallographic **b** direction. These feldspars show con-

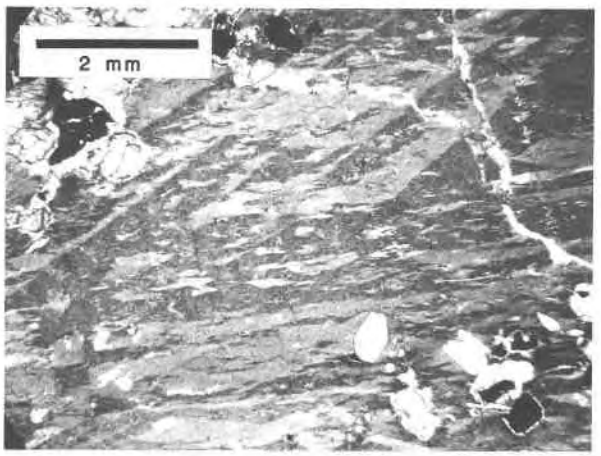

Fig. 16. Larvikite feldspar showing discontinuous nucleation of K-feldspar along diagonal plagioclase facets and flame structures growing along the composite sector (horizontal).

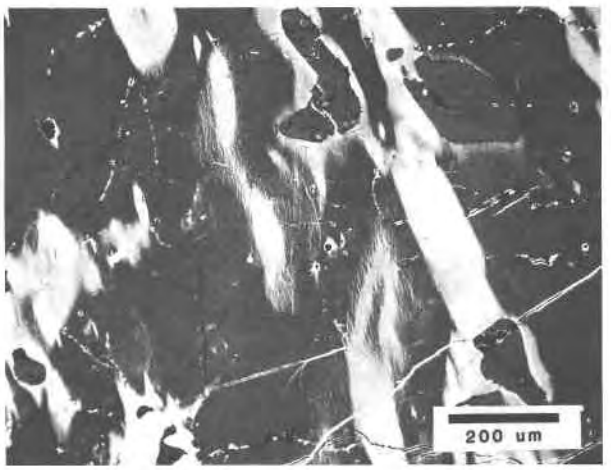

Fig. 17. Back-scattered electron image showing patchy intergrowth in a larvikite feldspar. Note incipient perthite exsolution next to the borders of the coarse intergrowth patches. White is K-feldspar; gray, albitic plagioclase; dark-gray clots, nepheline.

spicuously coarse segregations of oligoclase and K-feldspar (Petersen, 1985). The plagioclase component is generally heterogeneous, about $An_{15}Ab_{80}Or_5$, with variable Or content, whereas the K-feldspar is fairly homogeneous, about $An_5Ab_{50}Or_{45}$. Patchy intergrowths of the two phases produce a featherlike structure that demonstrates that the K-feldspar occurs predominantly in the lateral plane forming the sides of the feldspar dendrites and projecting toward the central stem (Fig. 15). Because these feldspars grow constrained preferentially along the **b** axis, the presence of composite plagioclase–alkali feldspar in the crystallographic **b** direction and predominant K-feldspar in the crystallographic **a** and **c** directions confirms that these data are in accord with the experimental observations presented here.

Because the patchy-intergrowth mechanism presented here is related to layer-spreading mechanisms, the development of directional, columnar growths is not an obligatory condition for the formation of patchy intergrowths. In fact, the main part of the Lardalite intrusion, as well as most larvikite occurrences, contains cumulus feldspars with intergrowth patterns that are similar to those of the columnar feldspars presented here. They display repeated, discontinuous occurrences of K-feldspar along distinct plagioclase facets and parallel growth in other crystallographic sectors (Fig. 16) and therefore may be the result of primary growth. Back-scattered electron images reveal that fine exsolution lamellae seem to increase toward the irregular K-feldspar-rich patches in accordance with greater ease of nucleation at this location (Fig. 17).

The results of the present study suggest that natural feldspar intergrowths, previously considered to be the result of solid-state exsolution reactions, may be at least in part the result of growth from the melt. This would clearly overcome some obvious difficulties in providing sufficiently slow cooling rates to allow solid-state diffusion to account for extremely coarse grained occurrences. The results also suggest that the considerably higher growth rates for this type solidification may lead to very coarse crystals with faceted outlines, in a fraction of the time that is usually indicated by growth rates of the single phases.

Conclusions

Coupled and noncoupled eutectic solidification occurs readily in ternary-feldspar melts at moderate cooling rates and near-cotectic conditions. The further the initial melt composition is removed from the cotectic, the more liquid fractionation is required to reach conditions for composite growth. Solute enrichment in a diffusive boundary layer at the primary plagioclase interface creates conditions for local supersaturation of sanidine and subsequent composite growth, before the bulk melt reaches cotectic composition.

The composite crystallization occurs primarily as a lamellar intergrowth of oligoclase and sanidine with a plane front and a much higher rate of growth than single phases. This growth is controlled by transverse diffusion across the interface and removal of latent heat of crystallization. Off-eutectic crystallization creates a diffusive boundary layer of solute-enriched liquid that can cause rhythmic compositional changes and banding during growth. The lamellar products show systematic compositional variations in the growth direction as well as gradual changes across individual facets following variations in the local supercooling.

A patchy intergrowth is formed when the preferential growth of sanidine in the crystallographic **a** and **c** directions is combined with simultaneous growth of a composite product in the crystallographic **b** direction. Depending on the relative growth rates in these two directions, the product develops a featherlike structure that is dominated by either K-feldspar or plagioclase with subordinate amounts of sanidine intergrowth. Because of the simultaneous growth of two components in the noncoupled intergrowth, the boundaries between the constituent phas-

es are irregular and, unlike the coupled intergrowth, show no reference to particular crystallographic planes.

Eutectic, coupled and noncoupled growth in the experiments occurs over a wide range of temperature and compositional conditions likely to exist in many natural, plutonic environments at small supercooling. Strikingly similar intergrowth structures are found in the ternary-feldspar larvikite of the Oslo region, Norway, and support the suggestion that many coarse feldspar intergrowths may indeed be the result of comparatively rapid, primary growth from the melt at near-cotectic conditions.

References

Barker, D.S. (1970) Compositions of granophyre, myrmekite, and graphic granite. Geological Society of America Bulletin, 81, 3339–3350.

Barth, T.F.W. (1945) Studies on the igneous rock complex of the Oslo region. II. Systematic petrography of the plutonic rocks. Skrifter utgitt av det Norske Videnskaps-Akademi i Oslo. Matematisk-Naturvidenskapelige Klasse 1944, 9, 1–104.

Carstens, Harold. (1983) Simultaneous crystallization of quartz-feldspar intergrowths from the melt. Geology, 11, 339–341.

Chalmers, Bruce. (1964) Principles of solidification. Wiley, New York.

Croker, M.N., Baragar, D., and Smith, R.W. (1975a) Anomalous eutectic growth II. The relationships between faceted/non-faceted eutectic structures. Journal of Crystal Growth, 30, 198–212.

Croker, M.N., McParlan, M., Baragar, D., and Smith, R.W. (1975b) Anomalous eutectic growth I. The determination of the eutectic structures of Bi-$TlBi_2$, Bi-Sn, Sb-Pb and Sb-InSb using an accelerated growth technique. Journal of Crystal Growth, 229, 85–97.

Dowty, Eric. (1976a) Crystal structure and crystal growth: I. The influence of internal structure on morphology. American Mineralogist, 61, 448–459.

——— (1976b) Crystal structure and crystal growth: II. Sector zoning in minerals. American Mineralogist, 61, 460–469.

Elliott, R. (1977) Eutectic solidification. International Metals Reviews, 219, 161–186.

Fenn, P.M. (1979) On the origin of graphic intergrowths. Geological Society of America Abstracts with Programs, 11, 424.

Flemings, M.C. (1974) Solidification processing. McGraw-Hill, New York.

Gilmer, G.H. (1977) Computer simulation of crystal growth. Journal of Crystal Growth, 42, 3–10.

Gilmer, G.H., and Jackson, K.A. (1977) Computer simulation of crystal growth. In E. Kaldis and H.J. Scheel, Eds. Crystal growth and materials, 79–114. North Holland, Amsterdam.

Hartman, P. (1982) Crystal faces: structure and growth. Geologie en Mijnbouw, 61, 313–320.

Hibbard, M.J. (1979) Myrmekite as a marker between pre-aqueous and postaqueous phase saturation in granitic systems. Geological Society of America Bulletin, 90, 1047–1062.

Holloway, J.R. (1971) Internally heated pressure vessels. In G.C. Ulmer, Ed. Research techniques for high pressure and high temperature, 217–258. Springer-Verlag, New York.

Hughes, C.J. (1972) Note on the variability of granophyric texture. Geological Society of America Bulletin, 83, 2419–2422.

Hunt, J.D., and Hurle, D.T.J. (1968) The structures of faceted/nonfaceted eutectics. Metallurgical Society of AIME Transactions, 242, 1043–1047.

Hunt, J.D., and Jackson, K.A. (1967) The dendrite-eutectic transition. Metallurgical Society of AIME Transactions, 239, 864–867.

Hurle, D.T.J., and Hunt, J.D. (1968) Structure of directionally solidified semiconductor eutectics. The solidification of metals, Iron and Steel Institute Publication 110, 162–166.

Jackson, K.A. (1958) Interface structure. In R.H. Doremus, B.W. Roberts, and P. Turnbull, Eds. Growth and perfection of crystals, 319–359. Wiley, New York.

——— (1984) Crystal growth kinetics. Materials Science and Engineering, 65, 7–13.

Jackson, K.A., and Hunt, J.D. (1966) Lamellar and rod eutectic growth. Metallurgical Society of AIME Transactions, 236, 1129–1142.

Kirkpatrick, R.J. (1981) Kinetics of crystallization of igneous rocks. In A.C. Lasaga and R.J. Kirkpatrick, Eds. Kinetics of geochemical processes, 321–398. Mineralogical Society of America Reviews in Mineralogy, 8.

Lofgren, G.E. (1974) An isothermal study of plagioclase crystal morphology: Isothermal crystallization. American Journal of Science, 274, 243–273.

——— (1980) Experimental studies on the dynamic crystallization of silicate melts. In R.B. Hargraves, Ed. Physics of magmatic processes, 487–551. Princeton University Press, Princeton, New Jersey.

——— (1983) Effect of heterogeneous nucleation on basaltic textures: A dynamic crystallization study. Journal of Petrology, 24, 229–255.

Lofgren, G.E., and Gooley, Ronald. (1977) Simultaneous crystallization of feldspar intergrowths from the melt. American Mineralogist, 62, 217–228.

Luth, W.C., and Ingamells, C.O. (1965) Gel preparation of starting materials for hydrothermal experimentation. American Mineralogist, 50, 255–258.

Mollard, F.R., and Flemings, M.C. (1967a) Growth of composites from the melt–Part I. Metallurgical Society of AIME Transactions, 239, 1526–1533.

——— (1967b) Growth of composites from the melt—Part II. Metallurgical Society of AIME Transactions, 239, 1534–1546.

Morris, L.R., and Winegard, W.C. (1969) The cell to dendrite transition. Journal of Crystal Growth, 6, 61–66.

Morse, S.A. (1968) Feldspars. Carnegie Institution of Washington Year Book 67, 120–126.

Morse, S.A., and Lofgren, G.E. (1978) Simultaneous crystallization of feldspar intergrowths from the melt: A discussion. American Mineralogist, 63, 419–421.

Muir, I.D., and Smith, J.V. (1956) Crystallization of feldspars in larvikites. Zeitschrift für Kristallographie, 107, 182–195.

Oftedahl, C. (1948) Studies on the igneous rock complex of the Oslo region. IX. The feldspars. Skrifter ugitt av det Norske Videnskaps-Akademi i Oslo. I Matematisk-Naturvidenskapelige Klasse 1948, 3, 1–129.

Petersen, J.S. (1985) Columnar-dendritic feldspars in the Lardalite intrusion, Oslo region, Norway: 1. Implications for unilateral solidification of a stagnant boundary layer. Journal of Petrology, 26, 223–252.

Rutter, J.W. (1977) Modification of eutectic morphology. Journal of Crystal Growth, 42, 515–525.

Smith, J.V. (1974) Feldspar minerals. 2. Chemical and textural properties. Springer-Verlag, New York.

Smith, J.V., and Muir, I.D. (1958) The reaction sequence in larvikite feldspars. Zeitschrift für Kristallographie, 110, 11–20.

Swanson, S.E. (1976) Growth of quartz crystals from silicate melts and the origin of graphic granite texture. (abs.) EOS (Amerian Geophysical Union Transactions), 57, 340.

——— (1977) Relation of nucleation and crystal-growth rate to the development of granitic textures. American Mineralogist, 62, 966–978.

Tiller, W.A., Jackson, K.A., Rutter, J.W., and Chalmers, B. (1953) The redistribution of solute atoms during the solidification of metals. Acta Metallurgica, 1, 428–437.

Yoder, H.S., Stewart, D.B., and Smith, J.V. (1957) Ternary feldspars. Carnegie Institution of Washington Year Book 56, 206–214.

Manuscript received March 29, 1985
Manuscript accepted November 15, 1985